Direct Patterning of Protein- and Cell-Resistant Polymeric Monolayers and Microstructures**

By *Ali Khademhosseini*, *Sangyong Jon*, *Kahp Y. Suh*, *Thanh-Nga T. Tran*, *George Eng*, *Judy Yeh*, *Jiehyun Seong*, and *Robert Langer**

Techniques that control topographical features and spatial presentation of surface molecules are important for the development of cell and protein arrays for drug discovery, diagnostic assays, and biosensors.[1] Cells and proteins have been previously patterned on various substrates using self-assembled monolayers (SAMs),[2–8] metal templates,[9] stamped proteins and peptides,[10] bio-[11–14] and comb polymers,[15] microfluidic channels,[16] and membranes.[17,18] Although these techniques may result in changes in surface topography based on deposition of a patterned molecule,[15–18] various properties of these features, such as height, are typically uncontrolled. To obtain features with controlled topographical features, techniques such as micromachining,[1] photolithography,[19] or molding[20,21] have been used. Therefore, the development of simple approaches that control both surface topography and spatial presentation of surface molecules for large-area substrates over a variety of feature sizes and heights is beneficial. Here, we describe a simple process that can be used to pattern oxide-based substrates with biofouling-resistant polymers with precise control over surface topography. The technique uses a molding process to pattern a poly(ethylene glycol) (PEG)-based random copolymer, poly((3-trimethoxysilyl)-propyl methacrylate)-*ran*-poly((ethylene glycol) methyl ether methacrylate) (poly(TMSMA-*r*-PEGMA)), in the form of polymeric monolayers (PMs) or microstructures with simple modifications to the fabrication procedure. We demonstrate the use of this technique to generate features varying in height and show its application for patterning proteins and cells.

PEG-based surface modification is widely used for creating surfaces that resist cells and proteins. For example, PEG-derived alkanethiol SAMs[2–4,7] have been used to pattern proteins and cells on gold substrates. While surface patterning through SAMs on gold is well characterized, stable patterning on other substrates is still under development. Recently, polyionic PEG-grafted polymers have been patterned on oxide surfaces using electrostatic interaction between cationic polymer backbone and anionic oxide surfaces.[22] However, the non-covalent interactions in this system may hinder its stability for long-term application. Furthermore, PEG-based alkanethiol SAMs cannot be used to create microstructures. To create PEG microstructures, photolithographic methods have been used.[19,23] However, the cost and complexities associated with photolithography provides a barrier to its widespread application for cell and protein patterning. In another approach, polymeric deposition of a PEG-based comb polymer was used to generate topographical changes, but no direct control over feature height was demonstrated.[15] To address the issues associated with stability, cost, topography, and ease of use, and control over feature height, we synthesized a poly(TMSMA-*r*-PEGMA) copolymer that can be easily synthesized using commercially available monomers. Detailed characteristics of this polymer are described elsewhere.[24] This copolymer provides the functionality of PEG (i.e., hydrophilic and non-biofouling), yet it can bind covalently with oxide surfaces to form monolayers or crosslink to form three-dimensional (3D) structures. Thus by utilizing the combination of this polymer and capillary force lithography, we have developed a universal approach to create features of varying sizes and shapes that could be applicable for patterning proteins and cells.

In capillary force lithography, direct contact of a patterned polydimethylsiloxane (PDMS) stamp on a mobilized polymer film provides the basis for pattern formation.[20,21] When a PDMS stamp is placed on a wet polymer film, the polymer spontaneously moves into the void space as a result of capillary action, thus forming a negative replica of the stamp. The technique generally consists of three steps: placing a PDMS stamp on the surface of a spin-coated polymer film, allowing the stamp to absorb solvent, and then letting the stamp and the substrate remain undisturbed for a period of time. When the film thickness is relatively thin with respect to the stamp's step height and the feature size is relatively large, instead of rising into the void space, the polymer migrates to the edge of the stamp and is localized there as a result of meniscus breakdown.[25] From a thermodynamic standpoint, this process can be interpreted to minimize the contact with the stamp and the substrate, which has been observed for other polymer systems.[25,26] As the stamp has the feature size that is typically of the order of 10–100 μm for patterning biological species, the dewetting would occur throughout the molding process.

For patterning, thin films of the poly(TMSMA-*r*-PEGMA) were spin-coated onto silicon oxide surfaces (typically wafers or glass slides). Immediately after coating, a PDMS mold was placed on the substrate to form a reversible seal (see Scheme 1). For these experiments we used PDMS molds with evenly spaced receding cylinders (ranging from 15 to 150 μm in diameter and 80 μm in height). As reported previously,[21] this capillary action is completed within a few minutes, which prevents the formation of a PM at the dewetted regions. In the course of the capillary action and solvent evaporation, the polymer within the void space spontaneously migrated to the

[*] Prof. R. Langer, A. Khademhosseini
Division of Biological Engineering
Massachusetts Institute of Technology
Cambridge, MA 02142 (USA)
E-mail: rlanger@mit.edu
Prof. R. Langer, Dr. S. Jon, Dr. K. Y. Suh, G. Eng, J. Yeh, J. Seong,
Department of Chemical Engineering
Massachusetts Institute of Technology
Cambridge, MA 02142 (USA)
Prof. R. Langer, Dr. T.-N. T. Tran
Harvard-MIT Division of Health Sciences and Technology
Cambridge, MA 02139 (USA)

[**] This research has been supported by NIH (NIH grant # HL60435) and NSF (through Bioprocess Engineering Research Center). AK is partially funded through a post graduate fellowship (PGS-B) from Natural Sciences and Engineering Research Council of Canada.

 DOI: 10.1002/adma.200305433

ADVANCED MATERIALS

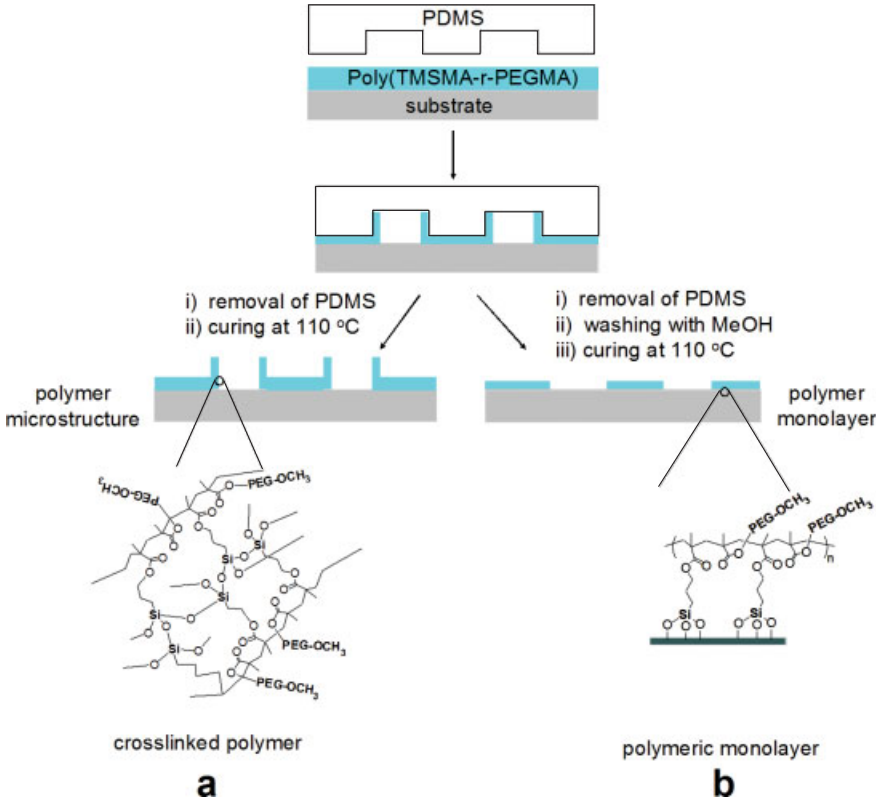

Scheme 1. Schematic diagram of the patterning process. Thin films of poly(TMSMA-*r*-PEGMA) were spin-coated on silicon oxide substrates and molded using capillary-force lithography. After 1 h, PDMS molds were detached from the substrate. To form microstructures, patterned substrates were immediately cured, which crosslinked the polymer and formed stable microstructures (a). To obtain PMs, patterned substrates were washed with methanol and then cured. A thin patterned layer of PEG-based polymer remained on the substrate due to covalent bonding to the substrate (b).

PDMS wall, with the substrate surface completely exposed, forming an additional physical barrier into the replicated pattern.[25,26] At the same time, the polymer that is in contact with the substrate reacts with the exposed silicon oxide, resulting in a robust, stable interface. The topographical features of the physical barrier are determined by the initial film thickness and PDMS feature width.[25] For example, the height of the barrier increases with increasing film thickness and decreasing feature width. The PDMS molds were kept on glass slides for 1 h since we have observed that complete coverage of the surface is reached within that time.[24] Upon removal of the PDMS mold, the pattern is visible by the naked eye. This pattern can then be further processed to obtain either microstructures or PMs.

To prepare polymeric microstructures with controlled topographical features, PDMS stamps were removed and the patterns were cured at 110 °C and then rinsed with methanol and water (Scheme 1a). During the curing step, polymer chains are cross-linked with each other through partially hydrolyzed trimethoxysilyl groups and form stable microstructures. Alternatively, patterned surfaces were first washed in methanol to remove unreacted polymer, leaving behind a thin polymer coating and then cured to obtain patterned PMs (Scheme 1b).

To demonstrate the feasibility of this approach to form both monolayers and microstructures, oxide substrates were patterned with a solution of poly(TMSMA-*r*-PEGMA) in methanol (5 mg mL^{-1}). Samples that were initially washed and then cured did not form visible patterns under light microscopy, whereas samples that were cured immediately after removal of the PDMS stamp, formed visible patterns (data not shown). In these samples, a sharp boundary separated the exposed substrate from the polymer-coated regions. To further examine these differences, atomic force microscopy (AFM) measurements were performed (Fig. 1). AFM images indicate that the thickness of PMs was ~1 nm (Fig. 1a,b), which was confirmed independently using ellipsometry (12 ± 4 Å). In contrast, samples that had not been previously washed formed a much rougher and thicker film of ~6 nm (60 ± 7 Å). This film surrounded a 40–70 nm high structure, which formed a boundary between the exposed substrate and the polymer film. This ring shaped structure, which had a typical aspect ratio of 5:1, was formed by the spontaneous dewetting of the polymer solution within the receding PDMS cylinders. After the PDMS stamp was removed, the polymer remained, forming the walls observed in Figure 1. The PMs formed in this study resembled those that we had previously characterized.[24] PMs were formed as a polymer monolayer on the surface stabilized by covalent bonds with the oxide surface. The methanol wash prior to crosslinking removed any non-surface reacted polymer, thus leaving a thin polymer film behind. Without thermal cross-linking, the thickness of this polymer film was not a function of time (up to 48 h),[24] thus thermal curing was required for the formation of thicker polymer films. In addition, this suggests that polymer crosslinking does not contribute greatly to the formation of the PM and that PM is stabilized by direct interaction with the surface.

To prepare features with higher topographical dimensions, we used 50 and 100 mg mL^{-1} polymer solutions. Higher poly(TMSMA-*r*-PEGMA) concentrations gave rise to morphologically distinct structures. At 50 mg mL^{-1}, the height of the polymeric structures surrounding each exposed region increased to 100–250 nm (Fig. 1a,b). As the polymer concentration was further increased to 100 mg mL^{-1}, the height of the structures increased to >450 nm. Thus, the height and shape of the wells were directly correlated to the polymer concentration, which is readily understood in terms of mass conservation. The ring microstructure became larger as the polymer content in the solution increased. It is expected that the height

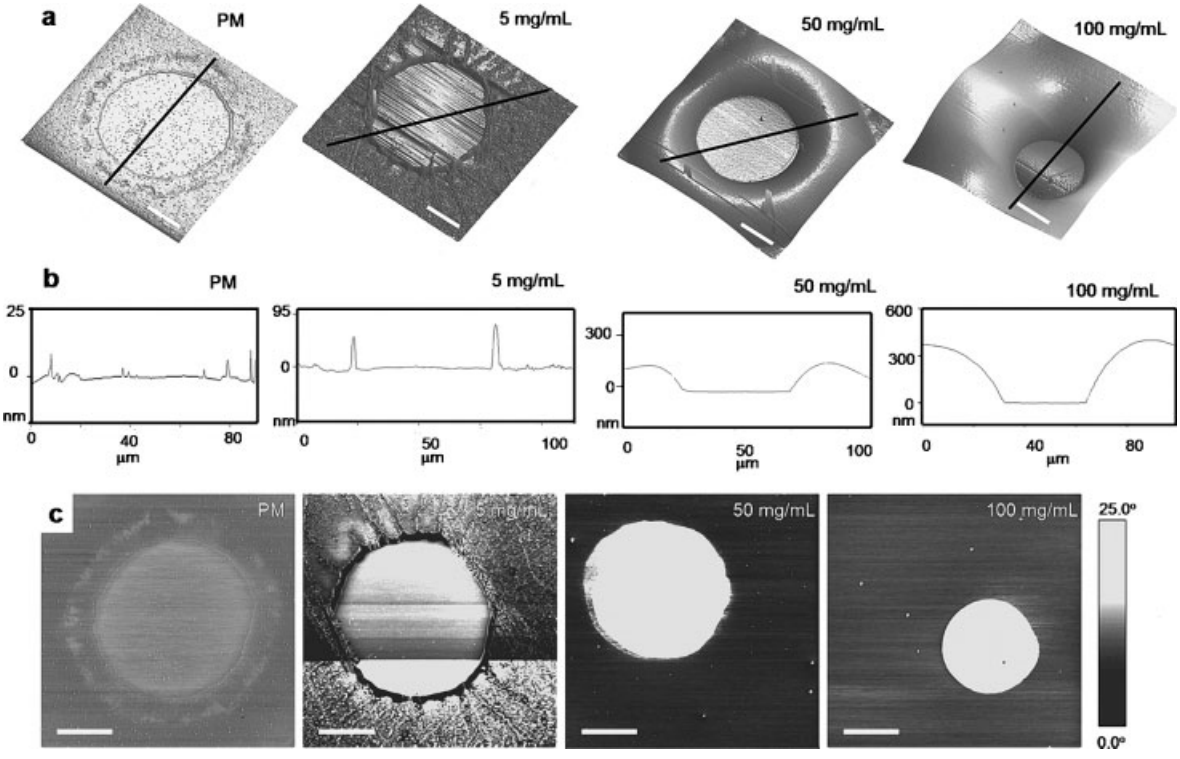

Fig. 1. AFM images of patterned surfaces using 5, 50, and 100 mg mL^{-1} poly(TMSMA-*r*-PEGMA) in methanol. PMs were prepared by washing the 5 mg mL^{-1} structures prior to curing; a) represents 3D rendering of the height image obtained for various samples; b) illustrates representative cross-sectional height images for various structures. The height and the shape of the structures formed were directly related to polymer concentration and fabrication technique. c) Phase images obtained from same samples as part (a). White bars indicate 20 μm.

of the features presented here would increase in aqueous solution due to PEG swelling in water, thus the values presented here provide lower limits of the topographical heights.

In addition, the inner diameter of the microwells formed in this approach was a function of the amount of deposited polymer, ranging from 50–60 μm for polymer concentrations up to 50 mg mL^{-1} to 30 μm for 100 mg mL^{-1} concentration (Fig. 1). It is expected that this approach can be utilized to control the feature size at a given length scale.

We also used AFM to determine the spatial distribution of surface molecules. Phase contrast in an AFM image indicates differences in the molecular interactions of the AFM tip with the surface, thus providing a measure of surface exposure. As illustrated in Figure 1c, a sharp phase contrast was observed using all conditions tested. Furthermore, the contrast intensity increased as the thickness of the polymer film increased, indicating a sharper difference in the surface properties of the exposed region and coated regions. This suggests that the regions within the ring-like structures were exposed to substrate and had not been coated by a thin polymeric layer.

To test the ability of the patterned surfaces to resist protein adsorption, patterned polymer microstructures or PMs were immersed in the solutions of fluorescein isothiocyanate (FITC)-labeled bovine serum albumin (BSA), FITC-labeled immunoglobin (IgG), and fibronectin (FN). Fluorescent images and quantitative analysis of the patterned surfaces demonstrate that BSA adhered to the co-polymer coated regions at ~4 % of the exposed substrate (Fig. 2a,b,e). Interestingly, higher polymer concentrations did not increase the protein resistant properties of the surrounding regions indicating that the surface coverage of the monolayers is comparable to that of thicker films. FN, a cell adhesive protein, was also selectively adhered to the exposed substrate for both PMs (Fig. 2c) and microstructures (Fig. 2d) at 2–3 % of the surrounding regions. Similarly, the increase in polymer concentration did not significantly influence the protein resistant properties of the surface. This may suggest the intrinsic polymer properties with regard to protein adsorption. Similar fluorescent images were also obtained for FITC-labeled IgG stained samples (data not shown). Protein adsorption was similar for a variety of pattern sizes as small as 15 μm in diameter over substrates up to ~2 cm × 3 cm, thus demonstrating that this technique is simple and efficient for patterning proteins.

To evaluate the feasibility of the patterned surfaces for selective cell attachment, NIH-3T3 fibroblasts were seeded on the patterned PMs and microstructures that had been pre-incubated with FN. As expected, NIH-3T3 cells selectively adhered to FN coated substrate within six hours after seeding for both PMs and microstructures (Fig. 3). Cells were patterned over large areas in a reproducible manner for all samples for various pattern sizes (ranging from 15 to 150 μm in diameter). The area of the exposed surface as well as cell seeding density determined the number of cells initially seeded per FN patch. Distinct differences were observed de-

ADVANCED MATERIALS

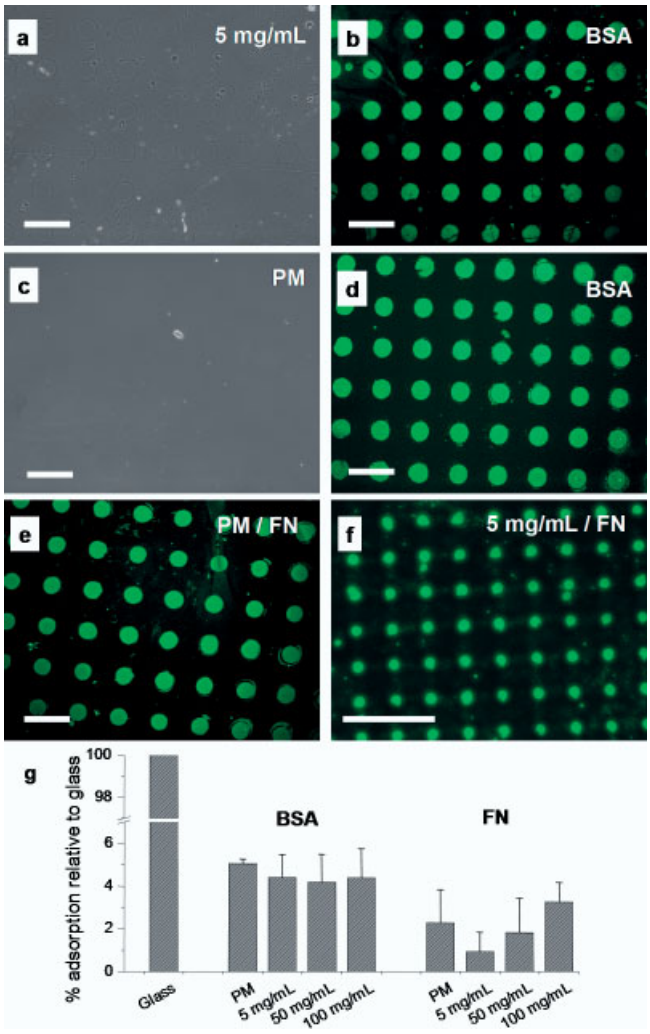

Fig. 2. BSA and FN adsorption onto poly(TMSMA-*r*-PEGMA) patterned on silicon oxide background. a,b) BSA staining of patterned microstructures (a) and PMs (b) for the same sections. c,d) FN staining micrographs for patterned PM (c) and microstructure (d). e) Quantitative values for the adsorption of FN and BSA on PEG-coated regions in comparison to the exposed substrate. Protein and BSA adhered selectively to the exposed substrate in comparison to the polymer coated regions. In addition, increasing polymer concentration did not enhance the protein resistant properties of the patterns. Bar indicates 200 μm.

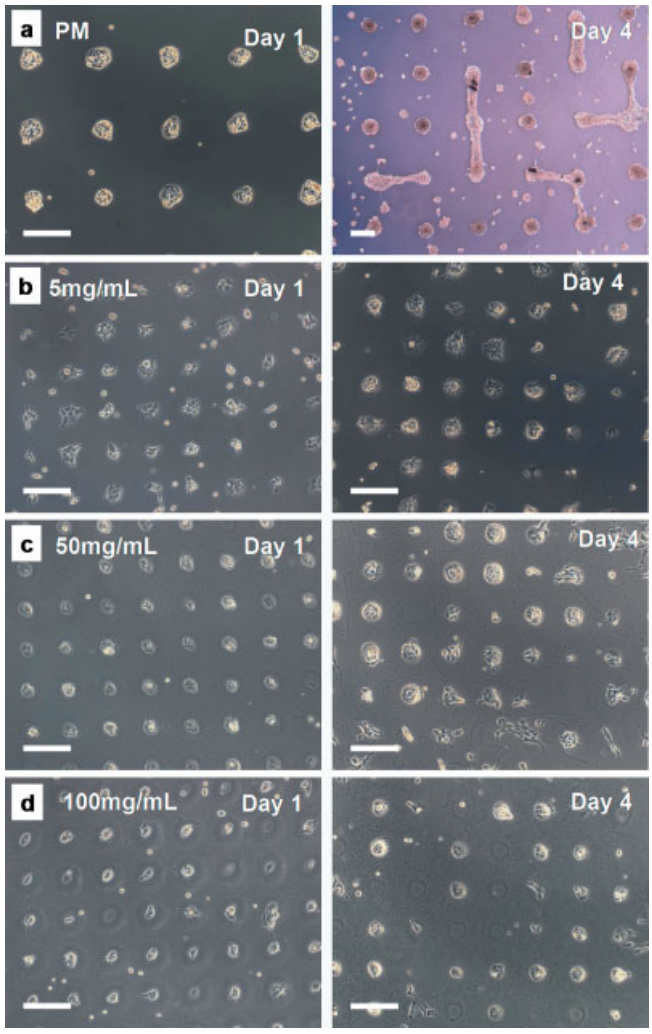

Fig. 3. NIH-3T3 cells on patterns of PM (a), 5 mg mL^{-1} (b), 50 mg mL^{-1} (c), and 100 mg mL^{-1} (d) polymer concentrations over time. The time at which the image was taken is shown in the figure. Bar indicates 200 μm.

pending on whether cells seeded were on PMs or in wells formed from microstructures. The most striking difference was the visible space between the cells and the walls of the microstructure. Thus, cells that were seeded within these wells remained confined to the bottom surface of the microwells and did not adhere to the polymeric walls.

Cells patterned on PMs were morphologically similar to previously obtained results by other groups.[4,7,8,27] For PM patterns, selective cell adhesion was driven by adhesion to FN and repulsion from PEG molecules, whereas for cells in microwells, the topographical features may have also contributed to cell patterning. As we demonstrated, the microstructures generated by this technique could range in size from 5 to > 500 nm, thus providing both an additional barrier to cell spreading and a favorable region for cells to deposit.

To determine the stability of these patterns, patterned cell arrays were tracked using phase contrast microscopy on PMs as well as on microstructures. Cell patterns on microstructures remained stable for at least 4 days (> 95 %) without many interconnections between adjacent cell islands (Fig. 3b,c,d). However, cell patterns on PMs were less stable (> 75 %) and started forming interconnections within four days (Fig. 3a). This behavior may be attributed to the effects of cell confinement within the microwells or PEG degradation of the monolayer, rather than incomplete initial coverage of the polymer (Fig. 2e).

A notable property of the current technique is the stability of the poly(TMSMA-*r*-PEGMA). Both the microwells and the PMs remained stable in water for at least two weeks. In addition, the microstructures were mechanically robust and could not be easily scratched from the substrate. Thus the cross-linking of the methoxysilyl groups in the polymer units can generate patterns that are mechanically and chemically stable under the tested conditions.

Although we have used a negative stamp in this paper, enhanced pattern fidelity can be ensured by using positive stamps. We have observed that positive stamps can be used to create patterns through minor alterations to the protocol. To ensure dewetting of contact regions between the PDMS and glass, surfaces were not plasma cleaned. In addition, water was used as the polymer solvent, which further repels PDMS and allows for pattern formation through dewetting. Patterns formed with positive stamps resemble the negative structures of the PDMS stamps with only slight deformations due to the presence of meniscus. This work is currently in progress and will be published at a later time.

In this paper we have patterned SiO_2-based substrates by taking advantage of the covalent bonding of a multivalent polymer. Moreover, the technique presented here can potentially be easily expanded to a variety of other substrates that can be modified to present surface reactive hydroxyl groups. The approach could also be expanded to a variety of tissue culture materials such as polystyrene and poly(methyl methacrylate) that have been treated with oxygen plasma. There are a number of possible advantages associated with this technique in comparison to the previously described methods of generating patterned surfaces. These include greater control over surface topography, ease in the synthesis of the polymer, and stability of the patterned features. This technique could be useful for applications that require control over both the topography as well as the molecular control of the surface. For example, this approach may be used to fabricate arrays of microwells with non-reactive walls for biological assays that desire molecules to react, hybridize or adsorb only to the bottom surface.

In conclusion, we present a novel method of patterning cells and proteins with a copolymer comprised of poly-anchoring groups. The technique allows for control over surface topography and surface molecules. The potential use of the technique for the development of improved biosensors and analytical tools is an area of active research.

Experimental

Polymer Synthesis: Poly(TMSMA-*r*-PEGMA) was synthesized and characterized as previously described [24]. Briefly, 3-(trimethoxysilyl)propyl methacrylate (Aldrich) and PEG methyl ether methacrylate (Aldrich) were reacted at a 1:1 molar ratio using free radical polymerization in tetrahydrofuran (THF) using 0.01 equivalents of 2,2′-azobisisobutyronitrile (AIBN) as initiator. The mixture was degassed for 20 min using Ar gas stream, after which the solution was sealed and placed at 70 °C for 24 h. After evaporation of solvent under vacuum, the polymer was obtained as a viscous liquid.

PDMS Mold Fabrication: PDMS molds were fabricated by curing prepolymer (Sylgard 184, Essex Chemical) on silicon masters that had been patterned with SU-8 photoresist. The patterns on the masters have protruding holes in the shape of cylinders (ranging in size from 20 μm to 160 μm), which result in PDMS replicas with receding cylinders. To cure the PDMS prepolymer, a mixture of 10:1 prepolymer and the curing agent was poured on the master and placed at 70 °C for 2 h. The PDMS mold was then peeled from the silicon wafer and plasma cleaned for 5 min prior to use.

Patterning Technique: To pattern the polymer onto substrate, a solution of co-polymer dissolved in methanol (ranging from 5 to 100 mg mL^{-1}) was spin-coated at 1000 rpm (rpm = revolutions per minute) for 10 s on a plasma cleaned glass substrate. A plasma cleaned PDMS mold was then immediately brought in conformal contact with the copolymer surface and stored at room temperature for 1 h. Molds were then detached from the glass substrate. To obtain PMs, the patterned surfaces were washed with methanol for 1 h and subsequently cured at 110 °C for 15 min. To obtain the polymeric microstructures, the patterns left from the PDMS mold were directly cured at 110 °C for 15 min.

Protein Adsorption: FITC-labeled BSA, FITC-labeled IgG and FN (Sigma) were dissolved in phosphate buffered saline (PBS) (Sigma) at 50 μg mL^{-1}, 50 μg mL^{-1}, and 20 μg mL^{-1} respectively. To test for BSA and IgG protein adhesion, a few drops of the protein solution was evenly distributed onto the patterned substrates and stored at room temperature for 30 min. The patterned substrates were then washed and directly analyzed under fluorescent microscope (Axiovert 200, Zeiss). To coat with FN, surfaces were dipped into FN solution for 15 min. To measure FN adhesion, the surfaces were stained with anti-FN antibody (Sigma) for an additional 45 min, followed by 1 h incubation with the FITC-labeled anti-rabbit secondary antibody. The surfaces were then washed with water and analyzed. Fluorescent images were quantified using Scion Image software. Pixel intensities were averaged for various regions for at least 2 independent experiments. Unstained glass slides that were analyzed at same exposure were used as negative controls.

Cell Culture: NIH-3T3 cells were maintained in 10 % fetal bovine serum (FBS) in Dulbecco's modified eagle medium (DMEM) at 37 °C and 5 % CO_2. For cell attachment experiments, the cells were trypsinized and washed and directly seeded on the patterned surfaces in serum containing medium at a cell density of ~ 10^4 cells cm^{-2}. Cell attachment to the patterned substrates was subsequently examined under a phase-contrast microscope at various times. To analyze, glass slides were rinsed with PBS to remove non-adhered cells from the non-adherent regions.

Atomic Force Microscopy: Scanning force microscopy (SEM) images (90 μm ×90 μm) were performed in tapping mode on a NanoScope III Dimension instrument (Digital Instruments) in air, using NSC15 tips (MikroMasch) at a scan rate of 0.25 Hz. Some of the images shown were flattened but not further manipulated.

Ellipsometry: Thickness measurements were carried out on an ellipsometer (Gaertner). Optical constants were measured prior to deposition and used to calculate thickness of the PEG layer after deposition. The maximum variation in the measured thickness between 3–4 spots on any sample was ±8 Å. Reported thicknesses are the average of at least two independent experiments where each sample was characterized by ellipsometry for at least three different locations on its surface.

Received: May 23, 2003
Final version: September 15, 2003

[1] T. Chovan, A. Guttman, *Trends Biotechnol.* **2002**, *20*, 116.
[2] R. Singhvi, A. Kumar, G. P. Lopez, G. N. Stephanopoulos, D. I. Wang, G. M. Whitesides, D. E. Ingber, *Science* **1994**, *264*, 696.
[3] M. Mrksich, G. M. Whitesides, *Annu. Rev. Biophys. Biomol. Struct.* **1996**, *25*, 55.
[4] M. Mrksich, L. E. Dike, J. Tien, D. E. Ingber, G. M. Whitesides, *Exp. Cell Res.* **1997**, *235*, 305.
[5] G. M. Whitesides, E. Ostuni, S. Takayama, X. Jiang, D. E. Ingber, *Annu. Rev. Biomed. Eng.* **2001**, *3*, 335.
[6] K. L. Prime, G. M. Whitesides, *Science* **1991**, *252*, 1164.
[7] M. Mrksich, C. S. Chen, Y. Xia, L. E. Dike, D. E. Ingber, G. M. Whitesides, *Proc. Natl. Acad. Sci. USA* **1996**, *93*, 10775.
[8] C. S. Chen, M. Mrksich, S. Huang, G. M. Whitesides, D. E. Ingber, *Science* **1997**, *276*, 1425.
[9] C. O'Neill, P. Jordan, P. Riddle, G. Ireland, *J. Cell Sci.* **1990**, *95*, 577.
[10] J. Hyun, Y. J. Zhu, A. Liebmann-Vinson, T. P. Beebe, A. Chilkoti, *Langmuir* **2001**, *17*, 6358.
[11] S. N. Bhatia, U. J. Balis, M. L. Yarmush, M. Toner, *Biotechnol. Prog.* **1998**, *8*, 378.
[12] S. N. Bhatia, U. J. Balis, M. L. Yarmush, M. Toner, *J. Biomater. Sci. Polym. Ed.* **1998**, *9*, 1137.
[13] S. N. Bhatia, M. L. Yarmush, M. Toner, *J. Biomed. Mater. Res.* **1997**, *34*, 189.
[14] S. N. Bhatia, U. J. Balis, M. L. Yarmush, M. Toner, *FASEB J.* **1999**, *13*, 1883.
[15] J. Hyun, H. Ma, Z. Zhang, T. P. Beebe, A. Chilkoti, *Adv. Mater.* **2003**, *15*, 576.
[16] S. Takayama, J. C. McDonald, E. Ostuni, M. N. Liang, P. J. A. Kenis, R. F. Ismagilov, G. M. Whitesides, *Proc. Natl. Acad. Sci. USA* **1999**, *96*, 5545.
[17] E. Ostuni, R. Kane, C. S. Chen, D. E. Ingber, G. M. Whitesides, *Langmuir* **2000**, *16*, 7811.
[18] A. Folch, B. H. Jo, O. Hurtado, D. J. Beebe, M. Toner, *J. Biomed. Mater. Res.* **2000**, *52*, 346.

ADVANCED MATERIALS

[19] A. Revzin, R. J. Russell, V. K. Yadavalli, W. G. Koh, C. Deister, D. D. Hile, M. B. Mellott, M. V. Pishko, *Langmuir* **2001**, *17*, 5440.
[20] K. Y. Suh, Y. S. Kim, H. H. Lee, *Adv. Mater.* **2001**, *13*, 1386.
[21] Y. S. Kim, K. Y. Suh, H. H. Lee, *Appl. Phys. Lett.* **2001**, *79*, 2285.
[22] L. A. Ruiz-Taylor, T. L. Martin, F. G. Zaugg, K. Witte, P. Indermuhle, S. Nock, P. Wagner, *Proc. Natl. Acad. Sci. USA* **2001**, *98*, 852.
[23] M. B. Chan-Park, Y. Yan, W. K. Neo, W. Zhou, J. Zhang, C. Y. Yue, *Langmuir* **2003**, *19*, 4371.
[24] S. Jon, J. Seong, A. Khademhosseini, T. T. Tran, P. E. Laibinis, R. Langer. *Langmuir* **2003**, in press.
[25] K. Y. Suh, P. J. Yoo, H. H. Lee, *Macromolecules* **2002**, *35*, 4414.
[26] K. Y. Suh, J. Park, H. H. Lee, *J. Chem. Phys.* **2002**, *116*, 7714.
[27] D. T. Chiu, N. L. Jeon, S. Huang, R. S. Kane, C. J. Wargo, I. S. Choi, D. E. Ingber, G. M. Whitesides, *Proc. Natl. Acad. Sci. USA* **2000**, *97*, 2408.

Low-Temperature Electrodeposition of Room-Temperature Ultraviolet-Light-Emitting Zinc Oxide**

By *Masanobu Izaki*,* *Seiji Watase*, and *Hisaya Takahashi*

Ultraviolet-light-emitting materials are a key to the future of optoelectronics. They can be used in laser diodes, for lithography processes, for large-capacity memories, and as a sterilizing light source.[1–3] (0001)-oriented ZnO is a realistic candidate for a room-temperature ultraviolet-light-emitting material, because of its wide bandgap energy of 3.3 eV and high exciton binding energy of 59 meV. (0001)-oriented ZnO layers have been prepared by heteroepitaxial growth onto GaN and single-crystal aluminum oxide (sapphire) substrates with a lattice mismatch of 2.4 % for the (0001) ZnO/(0001) GaN and 18.3 % for the (0001) ZnO/(0001) Al_2O_3 systems, respectively. Because of the advantages of Si wafers in conventional integrated circuit technology, Si wafers have also been employed as a substrate in ultraviolet-light-emitting devices for industrial applications. Since the lattice mismatch between the (0001) ZnO plane and the (001) or (111) Si planes is very large, an interlayer, such as CaF_2, is indispensable for growing heteroepitaxial ZnO on Si wafers.[4] (0001)-oriented ZnO layers have been prepared with gas-phase deposition techniques such as sputtering molecular beam epitaxy (MBE) and laser ablation, in which heating above 673 K during and/or after the film deposition is necessary.[5–8] If low-temperature preparation could be achieved by a simple process, ZnO could be used for a greater number of applications in optoelectronics, e.g., in circuit boards with embedded devices.[9]

Electrodeposition of ZnO films, which has several advantages over gas-phase deposition techniques, has been demonstrated by Izaki and Omi[10] and by Peulon and Lincot.[11] Heteroepitaxial electrodeposition of a (0001)-oriented ZnO was reported on a single-crystalline Au substrate by Switzer and co-workers[12] and on a (0001)-GaN-coated (0001) sapphire substrate by Pauporte and Lincot.[13] Although much research has been carried out, room-temperature ultraviolet-light-emission from electrodeposited (0001)-oriented ZnO has not been realized to date. Here we report on the low-temperature electrodeposition of a high-quality, (0001)-oriented ZnO layer that emits ultraviolet light due to bound excitons at photon energies of 3.25–3.30 eV and visible light at 2.38–2.70 eV at room temperature. We used an electrodeposition technique with a nitrate reduction reaction in aqueous solution and a (111) Au-coated (100) Si wafer as the substrate for depositing the (0001)-oriented ZnO layer.

Figure 1 shows an X-ray diffraction (XRD) spectrum and pole figures of (10$\bar{1}$1) ZnO and (111) Au planes for a ZnO layer electrodeposited onto a Au-coated Si substrate at –0.6 V. Only

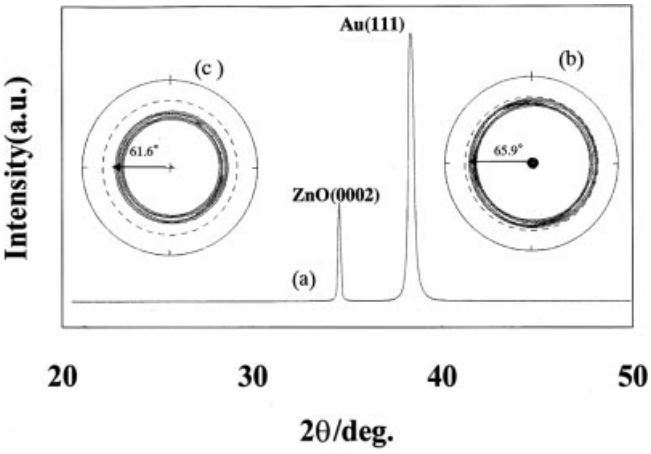

Fig. 1. a) XRD spectrum of a ZnO film prepared at –0.60 V, b) pole figure of Au(111), and c) pole figure of ZnO(10$\bar{1}$1) of the same film.

two peaks, assigned to the Au (111) and ZnO (0001) planes, could be observed. The Au layer with a face-centered cubic lattice had a (111) out-of-plane orientation with a random in-plane orientation, because the peaks at 0° and 65.9° on the (111) pole figure (Fig. 1b) could be assigned to equivalent planes of (111) orientation, and the intensity is distributed homogeneously along the azimuthal axis. ZnO layers electrodeposited at –0.50 to –0.80 V had a characteristic wurtzite structure with (0001) out-of-plane orientation and a random in-plane orientation, because a peak could be observed at a tilt angle of 61.6°, corresponding to the difference in angle of the (0001) and (10$\bar{1}$1) planes and the intensity was almost constant along the azimuthal axis on the (10$\bar{1}$1) pole figure (Fig. 1c). If ZnO has a [11$\bar{2}$0] in-plane orientation on a (0001) plane, six isolated peaks can be observed on the azimuthal axis of the ZnO (10$\bar{1}$1) pole figure.[12] The ZnO layers electrodeposited at –0.60 to –0.65 V showed an excellent (0001) preferred orientation in all the ZnO layers we prepared.

Figure 2 shows a cross-section of a (0001)-oriented ZnO layer electrodeposited at –0.60 V, taken with a field-emission

[*] Dr. M. Izaki, S. Watase
Department of Inorganic Chemistry
Osaka Municipal Technical Research Institute
1-6-50 Morinomiya, Joto-ku, Osaka 536-8553 (Japan)
E-mail: izaki@omtri.city.osaka.jp
H. Takahashi
Graduate School of Engineering, Utsunomiya University
7-1-1 Yoto, Utsunomiya-shi, Tochigi 321-8585 (Japan)

[**] We express our thanks to H. Inoue and T. Nagayama for their help with X-ray measurements and SEM observations.

  DOI: 10.1002/adma.200305465 *Adv. Mater.* **2003**, *15*, No. 23, December 3